Reverse-feeding effect of epidemic by propagators in two-layered networks*

Dayu Wu(吴大宇), Yanping Zhao(赵艳萍), Muhua Zheng(郑木华), Jie Zhou(周杰), and Zonghua Liu(刘宗华)†

Department of Physics, East China Normal University, Shanghai 200062, *China*

(Received 4 September 2015; revised manuscript received 10 October 2015; published online 20 December 2015)

Epidemic spreading has been studied for a long time and is currently focused on the spreading of multiple pathogens, especially in multiplex networks. However, little attention has been paid to the case where the mutual influence between different pathogens comes from a fraction of epidemic propagators, such as bisexual people in two separated groups of heterosexual and homosexual people. We here study this topic by presenting a network model of two layers connected by impulsive links, in contrast to the persistent links in each layer. We let each layer have a distinct pathogen and their interactive infection is implemented by a fraction of propagators jumping between the corresponding pairs of nodes in the two layers. By this model we show that (i) the propagators take the key role to transmit pathogens from one layer to the other, which significantly influences the stabilized epidemics; (ii) the epidemic thresholds will be changed by the propagators; and (iii) a reverse-feeding effect can be expected when the infective rate is smaller than its threshold of isolated spreading. A theoretical analysis is presented to explain the numerical results.

Keywords: propagators, complex network, two pathogens, epidemic spreading

PACS: 87.18.Yt, 05.45.Xt, 87.18.Sn **DOI:** 10.1088/1674-1056/25/2/028701

1. Introduction

Epidemic spreading has been a challenging problem for a long time as it usually causes major public health threats owing to their potential mortalities and substantial economic impacts. Its recent examples are the outbreaks of global infectious diseases including SARS (Severe Acute Respiratory Syndrome), H1N1 (Swine Influenza), H5H1 (Avian Influenza), and Ebola, etc. To understand how epidemics spread in a system, which is a crucial step to preventing and controlling outbreaks, several models have been proposed such as the susceptible-infected-susceptible (SIS) and susceptible-infected-refractory (SIR) models, etc.,[1] where S, I, and R represent the susceptible, infected, and refractory individuals, respectively. Based on these models, it is revealed that the epidemic can be spread out only when its infection rate is greater than a threshold.

The study of epidemics has been a very hot research topic in recent decades, due to the fast progress in network science.[2,3] It is revealed that the stabilized epidemic depends on many factors such as the network structure, adopted immunization, received information, and chosen traveling, etc. For example, it was found that the epidemic spreading on scale-free networks has no epidemic threshold in the thermodynamic limit.[4–11] Different approaches of immunization will result in different effects of controlling an epidemic, such as the targeted immunization[12–14] and acquaintance immunization,[15,16] etc. Received information will make individuals take self-protective actions to protect themselves.[17–21] Epidemic spreading on one layer will asymmetrically interact with the communication on another layer.[22,23] Objective traveling of choosing the shortest path will accelerate the epidemic spreading,[24–28] in contrast to the random diffusion model where individuals randomly choose one of its neighboring nodes for diffusion.[29–33]

Currently, the study of epidemics is focusing on the multi-layered networks where a variety of dynamics can be investigated.[34–36] A great deal ofattention has been paid to the case of multiple pathogens, where two or more diseases spread in the same population and each person can be infected by two or more of them.[37–42] In fact, this case is more realistic. For example, it was revealed that the persons infected by HIV have a higher risk to be infected by other pathogens, including hepatitis, tuberculosis, and malaria.[43,44] It was also found that the incidence of tuberculosis was increased during the 1918–1919 Spanish flu.[45,46] These evidences show that infection by one pathogen can effectively influence the infection process by the other pathogen, which may be either competitive or cooperative for the same population of hosts. Focusing on the two-pathogen scenario, it has been found that the onset of a disease's outbreak is conditioned to the prevalence levels of the other disease. For the case of competitive (cooperative) interaction between two pathogens, the presence of one pathogen makes the other less (more) likely to spread.[37,42,44,47–50]

A typical but interesting case of multiple pathogens

*Project supported by the National Natural Science Foundation of China (Grant Nos. 11135001, 11375066, and 11405059) and the National Basic Key Program of China (Grant No. 2013CB834100).

†Corresponding author. E-mail: zhliu@phy.ecnu.edu.cn

© 2016 Chinese Physical Society and IOP Publishing Ltd

is sexually transmitted diseases, which can propagate in both heterosexual and homosexual networks of sexual contacts.[51,52] This problem has been recently considered by Sanz *et al.*[53] and our team.[54] Sanz *et al.* thoroughly studied extensions of the SIS and SIR models, based on the condition of constant infection rates. While we presented a unified framework to study both the cooperative and competitive interactions between two pathogens in multiplex networks, based on a new concept of a state-dependent infectious rate.[54] However, all these considerations ignore the effect of bisexual men, which is evidenced to increase the AIDS-related risk.[55,56] A study on the number of partners among U.S. bisexual men shows that bisexual men are the medium to connect the pathogens in the network of heterosexual men with the pathogens in the network of homosexual men.[55–59] Based on these evidences, we here study this problem by focusing on the role of bisexual individuals, i.e., connecting the heterosexual network and homosexual network. Thus, we present a two-layered network model without fixed links between the two layers, but with dynamic propagators to connect the two layers. This model is not only limited for sexually transmitted diseases, but also for other pathogens caused by traveling between different cities. In detail, we let each layer have a distinct pathogen and let the propagators have a chance to jump between the two layers at each time step, see Fig. 1. That is, without the propagators, the two layers will be completely separated. In this way, the coupling between the two layers is not by some persistent links as in each layer but by a new type of impulsive links, i.e., jumping. To the best of our knowledge, this is the first model to consider impulsive links. By this model we show that (i) the propagators take the key role to transmit pathogens from one layer to the other, which significantly influences stabilized epidemics; (ii) the epidemic thresholds will be changed by the propagators; and (iii) a reverse-feeding effect can be expected when the infective rate is smaller than its threshold of isolated spreading. A theoretical analysis is presented to explain the numerical results.

The rest of this paper is organized as follows. In Section 2, we introduce the model to study the effect of the propagators. Then in Section 3, we make numerical simulations to show how the propagators influence the spreading of the two pathogens, especially the epidemic thresholds. After that, we give a brief theoretical analysis to explain the numerical results in Section 4. Finally, we give discussions and conclusions in Section 5.

2. Model

Figure 1 shows the schematic figure of our model. For simplicity, the up ("layer 1") and down ("layer 2") layers are considered to be two independent random Erdös-Rényi networks[2] with sizes N_1 and N_2 and average degrees $\langle k_1 \rangle$ and $\langle k_2 \rangle$, respectively. We assume that there are totally m propagators in the network and they are initially half in the up layer and the other in the down layer. The propagators have a double identity. They will behave only as homosexual (heterosexual) people when they are at the homosexual (heterosexual) layer. At each time step, every propagator will have a probability p to jump from its layer to the other layer. To smoothly implement this jumping process, we randomly choose m nodes from each layer and let them be fixed as the host nodes for the propagators. When the propagators are staying at these host nodes, their connections to neighbors will be active (see the "red" nodes in Fig. 1); otherwise, their connections to neighbors will be inactive (see the "empty" nodes in Fig. 1). In this sense, we will initially choose $m/2$ occupied nodes for the propagators and $m/2$ "hole" nodes at each layer. We will always have $N_1 - m$ non-jumping nodes at the up layer and $N_2 - m$ non-jumping nodes at the down layer. We let a propagator from one layer and a hole node from the other layer form a corresponding pair of nodes, see those pairs of nodes connected by the dotted "red" lines between the two layers in Fig. 1 with the "arrow" being the jumping direction. That is, each propagator can jump only to its corresponding "hole" node.

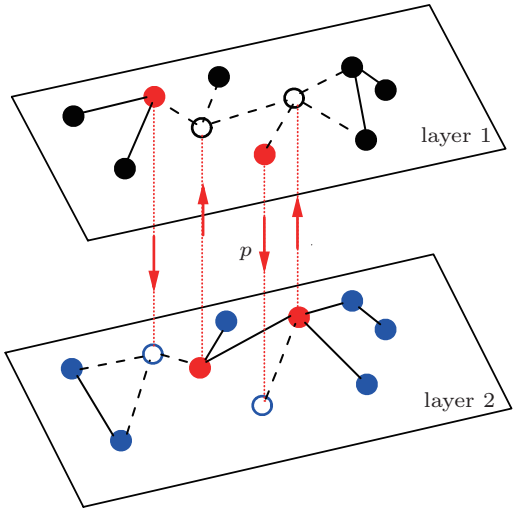


Fig. 1. (color online) Schematic figure of sexually transmitted diseases on a two-layered network where the up and down layers represent the networks of homosexual and heterosexual individuals, respectively, and are connected by the impulsive jumping of the bisexual individuals, called propagators. The "black" nodes represent the homosexual individuals, "blue" nodes the heterosexual individuals, the "red" nodes the bisexual individuals, and the "hole" nodes are for the jumping. The solid lines represent the active links while the dashed lines denote the inactive links. Each bisexual individual has a probability p to jump to its corresponding "hole" node at each time step.

Then, we assume two pathogens in the network, i.e., pathogen-1 on the up layer and pathogen-2 on the down layer. Without propagators, the two pathogens will independently spread on their individual layers, respectively. With propagators, the two pathogens will spread on both the two layers.

Therefore, there will be a dynamical interaction between the two pathogens once they spread to the same nodes. To understand how this dynamical interaction influences epidemic spreading, we here take the susceptible-infected-susceptible (SIS) model for both the two pathogens as an example. In the SIS model, a susceptible node may be infected by an infected neighbor at rate β when it contacts one infected node. At the same time, each infected node will become susceptible again at rate μ at each time step.[1,4,5,7,60–63] In the case of complex networks, a susceptible node may have $k_{\rm inf}$ infected neighbors, thus it will become infected with probability $1-(1-\beta)^{k_{\rm inf}}$. While the present case is more complicated as it has two interacting pathogens. To describe it, we let the set (S_1, I_1) represent pathogen-1 and the set (S_2, I_2) represent pathogen-2. In this case, a node will have 4 states: S_1S_2 — the node is susceptible to both pathogen-1 and pathogen-2; I_1S_2 — the node is infected by the first pathogen-1 but susceptible to pathogen-2; S_1I_2 — the node is susceptible to the first pathogen-1 but infected by the second pathogen-2; and I_1I_2 — the node is infected by both pathogen-1 and pathogen-2.[53,54]

Figure 2 shows the schematic illustration of the transition in the four status of a node, where the transition between S_1S_2 and I_1I_2 is ignored as a person will usually not be infected by two pathogens at exactly the same time. Let β_1 (β_2) and μ_1 (μ_2) be the infective and recovery rates of pathogen-1 (pathogen-2), respectively. Then, an S_1S_2 node will be infected into an I_1S_2 status by a probability $1-(1-\beta_1)^{k_{\rm inf1}}$, where $k_{\rm inf1}$ is the number of its total infected neighbors with either status I_1S_2 or status I_1I_2. At the same time, each I_1S_2 node will recover to the S_1S_2 status by a probability μ_1. Similarly, an S_1S_2 node will become the S_1I_2 status by a probability $1-(1-\beta_2)^{k_{\rm inf2}}$, where $k_{\rm inf2}$ is the number of its total infected neighbors with either status S_1I_2 or status I_1I_2. At the same time, each S_1I_2 node will recover to the S_1S_2 status by a probability μ_2.

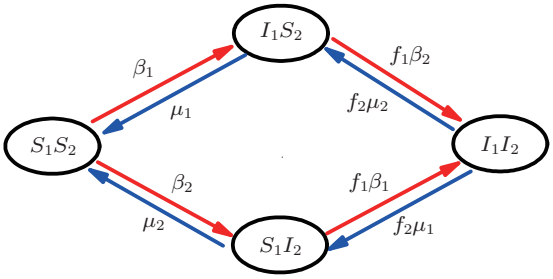


Fig. 2. (color online) Schematic illustration of the transition in the four status of a node, see the text for a detailed explanation.

For an infected node, its secondary infection by another pathogen will be different from its first infection. It has been revealed that an infection by malaria is shown to increase an individual's attractiveness to mosquitos,[64] which in turn may increase the chance to be infected by other strains. Generally, an infected person will become weakened and thus can be more likely to be attacked by another pathogen, which corresponds to the case of cooperation between two pathogens. On the other hand, when an infected person takes medicine, he will be less likely to get the other, which corresponds to the case of competition between two pathogens. We here introduce a factor to reflect this kind of cooperation or competition. In detail, we let f_1 be the infection factor and f_2 be the recovery factor. Thus, an I_1S_2 node will become the I_1I_2 status by a probability $1-(1-f_1\beta_2)^{k_{\rm inf2}}$. At the same time, each I_1I_2 node will recover to the S_1I_2 status by a probability $f_2\mu_2$. Similarly, an S_1I_2 node will become the I_1I_2 status by a probability $1-(1-f_1\beta_1)^{k_{\rm inf1}}$. At the same time, each I_1I_2 node will recover to the S_1I_2 status by a probability $f_2\mu_1$.

We are here mainly focused on how the impulsive jumping between the two networks influences the epidemic spreading, as it is what happens in reality and has not been paid attention so far. It is well known that the network topology will seriously influence the epidemic spreading.[2,3] To reduce the influence from the aspect of network topology, we limit the jumping probability to a very small range, i.e., $p \ll 1$. In this condition, the main influence between the two layers will come from the effect of jumping. We will use the random Erdös–Rényi networks as an example, as it is a good candidate for the mean-field approach. We find that the obtained results also work for other networks such as the scale-free networks.

3. Numerical simulations

In numerical simulations, we first construct two independent random Erdös–Rényi networks[2] as the up and down layers of Fig. 1, respectively. Notice that there are fewer homosexual people than heterosexual people, implying that the two networks in Fig. 1 will have different sizes. Thus, as an example, we here let the up network have $N_1 = 1000$ nodes and the down network have $N_2 = 4000$ nodes. To reflect the different ways of communication in the homosexual and heterosexual communities, we let the average degrees of the up network be $\langle k_{10}\rangle = 8$ and that of the down network be $\langle k_{20}\rangle = 3$. We let the number of total propagators be $m = 400$, i.e., there are initially $m/2 = 200$ propagators in each of the up and down layers. The non-jumping nodes will be 600 in the up layer and 3600 in the down layer. When the jumping probability p is zero, the up and down networks become independent. Notice that the links of the hole nodes in Fig. 1 are inactive. When the hole nodes are not neighboring each other, we have $\langle k_{10}\rangle m/2$ inactive links in the up network and $\langle k_{20}\rangle m/2$ inactive links in the down network. In general, it is possible for the hole nodes to also be neighbors of each other, indicating that the average degree of the up layer $\langle k_1\rangle$ will be less than $\langle k_{10}\rangle$ but greater than $(N_1\langle k_{10}\rangle - 2\langle k_{10}\rangle m/2)/(N_1 - m/2) = \langle k_{10}\rangle(N_1 - m)/(N_1 - m/2)$. Similarly, the average degree of the down layer $\langle k_2\rangle$ will be less than $\langle k_{20}\rangle$ but greater than

$\langle k_{20}\rangle(N_2-m)/(N_2-m/2)$. When the hole nodes are non-neighbors, we have $\langle k_1\rangle = \langle k_{10}\rangle(N_1-m)/(N_1-m/2) = 6$ and $\langle k_2\rangle = \langle k_{20}\rangle(N_2-m)/(N_2-m/2) \approx 2.84$. For a homogeneous random network, we have the critical infection rate $\beta_c = \mu/\langle k\rangle$.[65,66] Taking $\mu_1 = \mu_2 = 0.01$ as an example, we will have the thresholds $\beta_{1c0} \approx \mu/\langle k_1\rangle \approx 0.00167$ for the up layer and $\beta_{2c0} \approx \mu/\langle k_2\rangle \approx 0.00352$ for the down layer when the two layers are isolated with $p = 0$.

We now consider epidemic spreading by fixing $\mu_1 = \mu_2 = 0.01$ in this paper. We choose the factors $f_1 = 1.4$ and $f_2 = 1$, unless otherwise specified. Initially, we randomly choose a few nodes of the up (down) layer of Fig. 1 to be the infected seeds of pathogen-1 (pathogen-2). Then, we let the system evolve to a stabilized state and measure the density of infected nodes ρ_I, which includes both the first infection I_1S_2 or S_1I_2 and the secondary infection I_1I_2. We let ρ_I^{u1}, ρ_I^{u2} (ρ_I^{d1},ρ_I^{d2}) represent the densities of pathogen-1 and pathogen-2 in the up (down) layer, respectively, which exclude the hole nodes. Figure 3 shows the dependence of ρ_I on the jumping probability p with the "squares", "circles", "uptriangles", and "downtriangles" being ρ_I^{u1},ρ_I^{u2},ρ_I^{d1}, and ρ_I^{d2}, respectively, where panel (a) represents the case of $\beta_1 = 0.003$ and $\beta_2 = 0.005$, (b) the case of $\beta_1 = 0.003$ and $\beta_2 = 0.003$, (c) the case of $\beta_1 = 0.0014$ and $\beta_2 = 0.005$, and (d) the case of $\beta_1 = 0.0014$ and $\beta_2 = 0.003$. The parameters in Fig. 3 are chosen for four typical situations, i.e. $\beta_1 > \beta_{1c0}$ and $\beta_2 > \beta_{2c0}$ in panel (a), $\beta_1 > \beta_{1c0}$ and $\beta_2 < \beta_{2c0}$ in panel (b), $\beta_1 < \beta_{1c0}$ and $\beta_2 > \beta_{2c0}$ in panel (c), and $\beta_1 < \beta_{1c0}$ and $\beta_{1c0} < \beta_2 < \beta_{2c0}$ in panel (d). A common point in the four panels of Fig. 3 is that when $p = 0$, there is at most one pathogen of $\rho_I > 0$ for each layer, confirming the independence of the two layers at $p = 0$.

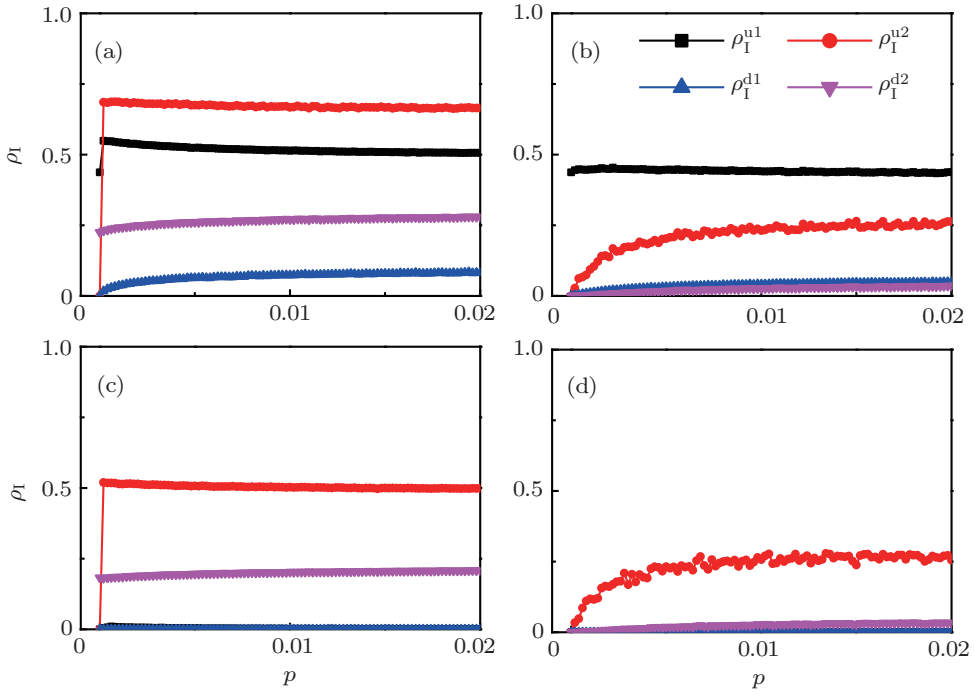


Fig. 3. (color online) Dependence of ρ_I on the jumping probability p with the "squares", "circles", "uptriangles", and "downtriangles" being ρ_I^{u1}, ρ_I^{u2}, ρ_I^{d1}, and ρ_I^{d2}, respectively, where panel (a) represents the case of $\beta_1 = 0.003 > \beta_{1c0}$ and $\beta_2 = 0.005 > \beta_{2c0}$, (b) the case of $\beta_1 = 0.003 > \beta_{1c0}$ and $\beta_2 = 0.003 < \beta_{2c0}$, (c) the case of $\beta_1 = 0.0014 < \beta_{1c0}$ and $\beta_2 = 0.005 > \beta_{2c0}$, and (d) the case of $\beta_1 = 0.0014 < \beta_{1c0}$ and $\beta_2 = 0.003 < \beta_{2c0}$ but with $\beta_2 > \beta_{1c0}$. The results are averaged over 1000 realizations.

The chosen values of $\beta_1 > \beta_{1c0}$ and $\beta_2 > \beta_{2c0}$ in Fig. 3(a) guarantee that both pathogen-1 and pathogen-2 can spread in their host layers when $p = 0$. When $p > 0$, the infected seeds of pathogen-1 (pathogen-2) will be transmitted to the down (up) layer and then cause its spreading there. In the up layer of the case of Fig. 3(a), both β_1 and β_2 are greater than β_{1c0} and thus they can both spread out, provided that the propagators can transmit the infected seeds of pathogen-2 from the down layer to the up layer. The final ρ_I^{u1} and ρ_I^{u2} are mainly determined by $\beta_1 - \beta_{1c0}$ and $\beta_2 - \beta_{1c0}$, which results in their approximate constant values in Fig. 3(a). While in the down layer, we have $\beta_1 < \beta_{2c0}$, thus the seeds of pathogen-1 cannot spread out but can only stay there for a transient time. As the recovery rate $\mu_2 = 0.01 < 1$, a transmitted seed of pathogen-1 will keep its status for some time steps before it jumps back to the up layer. In this sense, $p > 0$ will provide persistent jumping seeds of pathogen-1 into the down layer and thus the value of ρ_I^{d1} will be proportional to p. On the other hand, for an individual seed, its effect of epidemic spreading depends not only on the jumping speed but also on the contacting time,[25] resulting in a nonlinear dependence of ρ_I^{d1} on p, as in Fig. 3(a). Figures 3(b) and 3(c) can be similarly explained. Comparing

the corresponding values of ρ_I^{u2} in Figs. 3(c) and 3(a), we see that ρ_I^{u2} is about 0.5 in panel (c) and 0.7 in panel (a), indicating a significant difference. The reason is that there is no interaction between the two pathogens in Fig. 3(c) with $\rho_I^{u1} = 0$ but with interaction in Fig. 3(a) with $\rho_I^{u1} \approx 0.5$, indicating that the interaction has significantly influenced the spreading of the two pathogens.

We now turn to Fig. 3(d) with both $\beta_1 < \beta_{1c0}$ and $\beta_2 < \beta_{2c0}$. When $p = 0$, there are neither nonzero pathogen-1 nor nonzero pathogen-2 in the system. However, $p > 0$ induces an interesting phenomenon that ρ_I^{u2} and ρ_I^{d2} are both nonzero! This phenomenon can be explained as follows. The initial seeds of pathogen-2 will spread on the down layer for some time before its death. During this time period, the jumping propagators will have the chance to bring pathogen-2 into the up layer. As we have $\beta_2 > \beta_{1c0}$, the transmitted seeds of pathogen-2 will spread out on the up layer. Then, the propagators will send pathogen-2 back to the down layer and thus sustain the nonzero ρ_I^{d2} there, resulting in an interesting "reverse-feeding" phenomenon.

To understand the underlying mechanism of the nonlinear dependence of ρ_I on p in the four panels of Fig. 3, we divide its complicated dynamics into two aspects, i.e., the structure and mutual influence of two pathogens. Firstly, we focus on the aspect of structure, i.e., different average degrees between the up and down layers. To clearly see its effect, we consider the case of only one pathogen in the network. Figures 4(a) and 4(b) show the results of $\beta_2 = 0$, where panel (a) represents the case of $\beta_1 = 0.003 > \beta_{1c0}$ and panel (b) the case of $\beta_1 = 0.0014 < \beta_{1c0}$. From Fig. 4(a) we see that with the increase of p, ρ_I^{u1} is slightly decreased while ρ_I^{d1} increases from zero gradually. This result can be explained as follows. As $\beta_1 = 0.003 < \beta_{2c0}$, the epidemic cannot spread out at the down layer, indicating that ρ_I^{d1} is mainly obtained by the jumping process. In this sense, the increase of p will result in an increase of ρ_I^{d1}. At the same time, the jumping will make ρ_I^{u1} be slightly decreased. From Fig. 4(b) we see that both ρ_I^{u1} and ρ_I^{d1} are zero, which can be easily understood by $\beta_1 = 0.0014$ being smaller than both β_{1c0} and β_{2c0}.

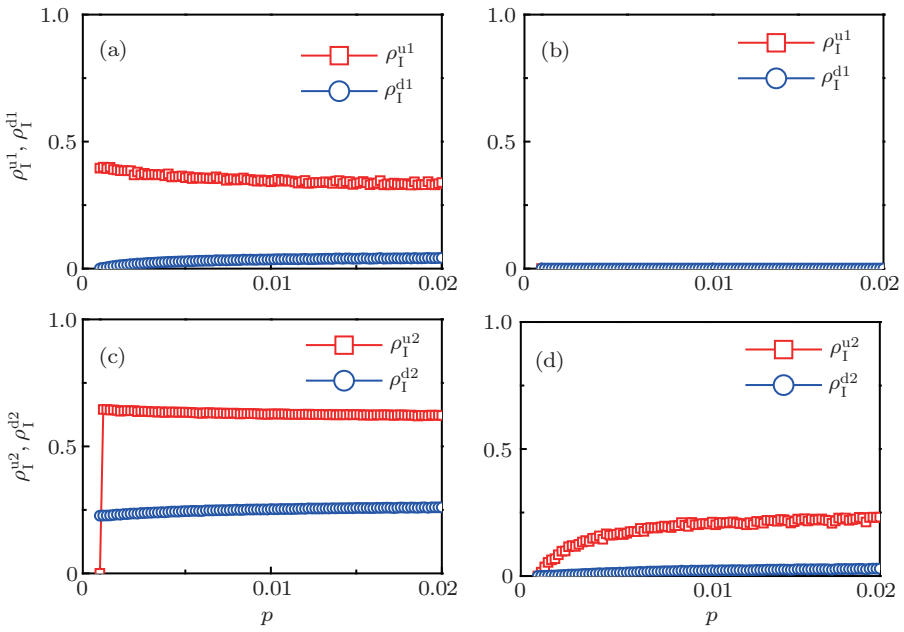


Fig. 4. (color online) Influence of structure difference of the two layers on epidemic spreading. Panels (a) and (b) show the case of $\beta_2 = 0$, where ρ_I^{u1} and ρ_I^{d1} represent the infected densities of pathogen-1 at the up and down layers, respectively. The parameter β_1 is chosen as $\beta_1 = 0.003 > \beta_{1c0}$ in panel (a) and $\beta_1 = 0.0014 < \beta_{1c0}$ in panel (b). Panels (c) and (d) show the case of $\beta_1 = 0$, where ρ_I^{u2} and ρ_I^{d2} represent the infected densities of pathogen-2 at the up and down layers, respectively. The parameter β_2 is chosen as $\beta_2 = 0.005 > \beta_{2c0}$ in panel (c) and $\beta_2 = 0.003 < \beta_{2c0}$ in panel (d).

Figure 4(c) and 4(d) show the results of $\beta_1 = 0$, where panel (c) represents the case of $\beta_1 = 0.005 > \beta_{2c0}$ and (d) the case of $\beta_2 = 0.003 < \beta_{2c0}$. From Fig. 4(c) we see that with the increase of p, both ρ_I^{u2} and ρ_I^{d2} are approximately constants. This result can be explained as follows. As $\beta_2 = 0.005$ is greater than both β_{2c0} and β_{1c0}, the epidemic can spread out at both the up and down layers. In this situation, ρ_I^{u2} will be determined by β_2–β_{1c0} and ρ_I^{d2} will be determined by $\beta_2 - \beta_{2c0}$. Thus, the influence of p can be ignored. Figure 4(d) shows a completely different case where both ρ_I^{u2} and ρ_I^{d2} increase with the increase of p but with $\rho_I^{u2} \gg \rho_I^{d2}$. The reason is that $\beta_2 = 0.003$ is smaller than β_{2c0} but greater than β_{1c0}. The condition of $\beta_2 < \beta_{2c0}$ will make the epidemic not be spread out, indicating no epidemic at both the up and down layers when $p = 0$. However, when $p > 0$, it is possible for pathogen-2 to be transmitted to the up layer by the propaga-

tors. Once it happens, pathogen-2 will spread out at the up layer because $\beta_2 > \beta_{1c0}$. Then the propagator will bring the infected ones back to the down layer and thus result in a sustained ρ_I^{d2}, i.e. "reverse-feeding" phenomenon, indicating that the effect of reverse-feeding is mainly from the difference of thresholds between β_{2c0} and β_{1c0} caused by the different average degrees between the up and down layers.

Secondly, we consider the aspect of mutual influence of two pathogens, where f_1 and f_2 are the two key parameters to determine the feature of interaction, i.e. cooperation or competition. To clearly see its effect, we focus on the influence of f_1 and f_2 on the epidemic thresholds. We let β_{1c} and β_{2c} be the epidemic thresholds of the up and down layers with $p > 0$, respectively. We first check the effect of f_1 by fixing $f_2 = 1$ and $p = 0.005$. Figure 5(a) shows how β_{1c} depends on f_1 where the "squares" and "uptriangles" represent the cases of $\beta_2 = 0.005$ and 0.003, respectively. From Fig. 5(a) we see that β_{1c} decreases with the increase of f_1 for the two cases but is faster in the case of $\beta_2 = 0.005$ than that of $\beta_2 = 0.003$. This result can be understood as follows. As $\beta_2 = 0.005$ is greater than both β_{1c0} and β_{2c0}, pathogen-2 can spread out in both the up and down layers, implying an interaction between the two pathogens in the up layer. Notice that an increase of f_1 means the enhanced cooperation between the two pathogens. Therefore, the increase of f_1 will result in an enhanced spreading of ρ_I^{u1} and thus a decreased β_{1c} on f_1. While in the case of $\beta_2 = 0.003$, its ρ_I^{u2} will be much smaller than that of $\beta_2 = 0.005$, indicating its interaction with ρ_I^{u1} will be much weaker than that of $\beta_2 = 0.005$ and thus will result in a slower decreased β_{1c} on f_1.

Figure 5(b) shows how β_{2c} depends on f_1 where the "squares" and "uptriangles" represent the cases of $\beta_1 = 0.003$ and 0.0014, respectively. From Fig. 5(b) we see that β_{2c} decreases with the increase of f_1 for the case of $\beta_1 = 0.003$ but keeps a constant for the case of $\beta_1 = 0.0014$. This result is easy to understand. As $\beta_1 = 0.003$ is greater than β_{1c0} but smaller than β_{2c0}, there will be a small quantity of ρ_I^{d1} at the down layer by the jumping process. Its interaction with ρ_I^{d2} will enhance the spread of pathogen-2 and thus result in a decreased β_{2c} on f_1. While $\beta_1 = 0.0014$ is smaller than both β_{1c0} and β_{2c0}, there will be no ρ_I^{d1} and thus no interaction with ρ_I^{d2}, resulting in a constant β_{2c}.

We now turn to check the effect of f_2 by fixing $f_1 = 1$ and $p = 0.005$. Figure 5(c) shows how β_{1c} depends on f_2 where the "squares" and "uptriangles" represent the cases of $\beta_2 = 0.005$ and 0.003, respectively. Figure 5(d) shows how β_{2c} depends on f_2 where the "squares" and "uptriangles" represent the cases of $\beta_1 = 0.003$ and 0.0014, respectively. Comparing Figs. 5(c) and 5(d) with Figs. 5(a) and 5(b), respectively, we see that their dependence on f_1 and f_2 is the opposite, confirming the role of the infection factor f_1 and the role of the recovery factor f_2.

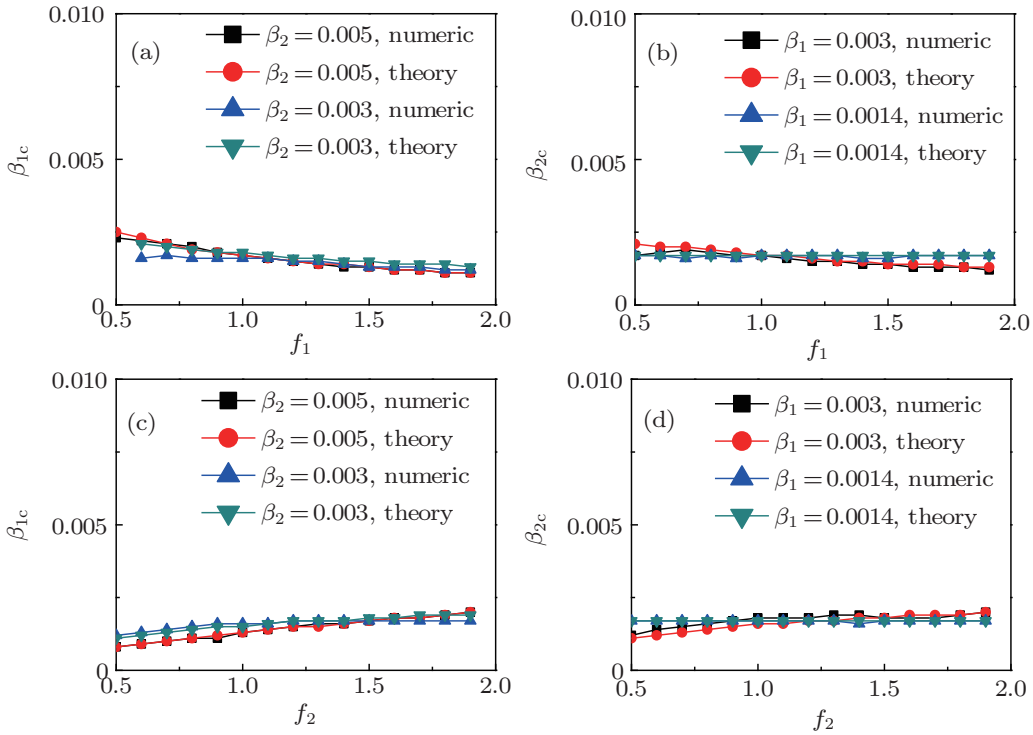


Fig. 5. (color online) Influence of f_1 and f_2 on the epidemic thresholds β_{1c} and β_{2c} with fixed $p = 0.005$, where the "squares" and "uptriangles" represent the numerical simulations and "circles" and "downtriangles" represent the corresponding theoretical results from Eqs. (2)–(5). (a) β_{1c} versus f_1 with $f_2 = 1$, where the "squares" and "uptriangles" represent the cases of $\beta_2 = 0.005$ and 0.003, respectively. (b) β_{2c} versus f_1 with $f_2 = 1$, where the "squares" and "uptriangles" represent the cases of $\beta_1 = 0.003$ and 0.0014, respectively. (c) β_{1c} versus f_2 with $f_1 = 1$, where the "squares" and "uptriangles" represent the cases of $\beta_2 = 0.005$ and 0.003, respectively. (d) β_{2c} versus f_2 with $f_1 = 1$, where the "squares" and "uptriangles" represent the cases of $\beta_1 = 0.003$ and 0.0014, respectively. The results are averaged over 1000 realizations.

Finally, we discuss how the parameter m influences the thresholds β_{1c} and β_{2c}. We fix the total numbers of nodes N_1 and N_2 and let $p = 0.005$, $f_1 = 1.4$, and $f_2 = 1$. When m increases, the non-jumping nodes in both the up and down layers will decrease by $N_1 - m$ and $N_2 - m$, respectively, which results in the decrease of $\langle k_1 \rangle$ and $\langle k_2 \rangle$ and then the increase of β_{1c} and β_{2c}. Figure 6 shows the results where the "squares" and "uptriangles" in panel (a) represent the cases of $\beta_2 = 0.005$ and 0.003, respectively, and the "squares" and "uptriangles" in panel (b) represent the cases of $\beta_1 = 0.003$ and 0.0014, respectively. From Fig. 6(a) we see that the line with "squares" is smaller than that of "uptriangles", implying that a larger β_2 has a stronger influence on the threshold β_{1c}. We see the same result in Fig. 6(b), indicating that a larger β_1 also has a stronger influence on the threshold β_{2c}.

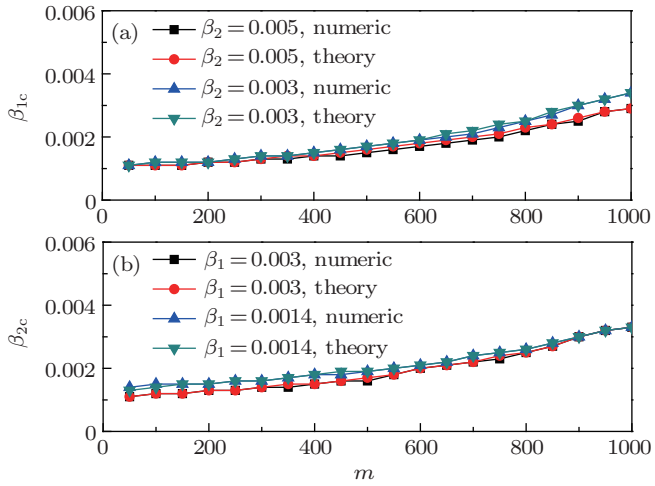


Fig. 6. (color online) Dependence of the thresholds β_{1c} and β_{2c} on m with fixed $p = 0.005$, $f_1 = 1.4$, and $f_2 = 1$, where the results are averaged over 1000 realizations. (a) β_{1c} versus m where the "squares" and "uptriangles" represent the cases of $\beta_2 = 0.005$ and 0.003, respectively, and "circles" and "downtriangles" represent the corresponding theoretical results, respectively. (b) β_{2c} versus m where the "squares" and "uptriangles" represent the cases of $\beta_1 = 0.003$ and 0.0014, respectively, and "circles" and "downtriangles" represent the corresponding theoretical results, respectively.

4. A brief theoretical analysis

We now conduct a theoretical analysis on the above numerical simulations. For convenience, we introduce ρ^{u}_{SS}, ρ^{u}_{IS}, ρ^{u}_{SI}, and ρ^{u}_{II} to represent the four densities of status [SS, IS, SI, II] in the up layer. Similarly, we let ρ^{d}_{SS}, ρ^{d}_{IS}, ρ^{d}_{SI}, and ρ^{d}_{II} to represent the four densities of status [SS, IS, SI, II] in the down layer. Thus, we have

$$\begin{aligned}
\rho_{I}^{u1} &= \rho^{u}_{IS} + \rho^{u}_{II}, \\
\rho_{I}^{u2} &= \rho^{u}_{SI} + \rho^{u}_{II}, \\
\rho_{I}^{d1} &= \rho^{d}_{IS} + \rho^{d}_{II}, \\
\rho_{I}^{d2} &= \rho^{d}_{SI} + \rho^{d}_{II}.
\end{aligned} \tag{1}$$

We divide the dynamics process into two steps, i.e. reaction and jumping. For the former, we use the mean-field approach to figure out the densities ρ_{SS}, ρ_{IS}, ρ_{SI}, and ρ_{II}. According to Fig. 2, the evolution equations of the two epidemics in the up layer can be given as

$$\begin{aligned}
\rho^{u}_{SS}(t+1) &= \rho^{u}_{SS} + \mu_1 \rho^{u}_{IS} + \mu_2 \rho^{u}_{SI} \\
&\quad - \langle k_1 \rangle \rho^{u}_{SS}[\beta_1(\rho^{u}_{IS} + \rho^{u}_{II}) + \beta_2(\rho^{u}_{SI} + \rho^{u}_{II})], \\
\rho^{u}_{IS}(t+1) &= \rho^{u}_{IS} - \mu_1 \rho^{u}_{IS} + \beta_1 \langle k_1 \rangle \rho^{u}_{SS}(\rho^{u}_{IS} + \rho^{u}_{II}) \\
&\quad + f_2 \mu_2 \rho^{u}_{II} - f_1 \beta_2 \langle k_1 \rangle \rho^{u}_{IS}(\rho^{u}_{SI} + \rho^{u}_{II}), \\
\rho^{u}_{SI}(t+1) &= \rho^{u}_{SI} - \mu_2 \rho^{u}_{SI} + \beta_2 \langle k_1 \rangle \rho^{u}_{SS}(\rho^{u}_{SI} + \rho^{u}_{II}) \\
&\quad + f_2 \mu_1 \rho^{u}_{II} - f_1 \beta_1 \langle k_1 \rangle \rho^{u}_{SI}(\rho^{u}_{IS} + \rho^{u}_{II}), \\
\rho^{u}_{II}(t+1) &= \rho^{u}_{II} + f_1 \beta_2 \langle k_1 \rangle \rho^{u}_{IS}(\rho^{u}_{SI} + \rho^{u}_{II}) - f_2 \mu_2 \rho^{u}_{II} \\
&\quad + f_1 \beta_1 \langle k_1 \rangle \rho^{u}_{SI}(\rho^{u}_{IS} + \rho^{u}_{II}) - f_2 \mu_1 \rho^{u}_{II},
\end{aligned} \tag{2}$$

where all the terms on the right-hand side of equations are taken at the time t. Obviously, they satisfy the conservation laws $\rho^{u}_{SS} + \rho^{u}_{IS} + \rho^{u}_{SI} + \rho^{u}_{II} = 1$. Similarly, we have the evolution equations of the two epidemics in the down layer as follows:

$$\begin{aligned}
\rho^{d}_{SS}(t+1) &= \rho^{d}_{SS} + \mu_1 \rho^{d}_{IS} + \mu_2 \rho^{d}_{SI} \\
&\quad - \langle k_2 \rangle \rho^{d}_{SS}[\beta_1(\rho^{d}_{IS} + \rho^{d}_{II}) + \beta_2(\rho^{d}_{SI} + \rho^{d}_{II})], \\
\rho^{d}_{IS}(t+1) &= \rho^{d}_{IS} - \mu_1 \rho^{d}_{IS} + \beta_1 \langle k_2 \rangle \rho^{d}_{SS}(\rho^{d}_{IS} + \rho^{d}_{II}) \\
&\quad + f_2 \mu_2 \rho^{d}_{II} - f_1 \beta_2 \langle k_2 \rangle \rho^{d}_{IS}(\rho^{d}_{SI} + \rho^{d}_{II}), \\
\rho^{d}_{SI}(t+1) &= \rho^{d}_{SI} - \mu_2 \rho^{d}_{SI} + \beta_2 \langle k_2 \rangle \rho^{d}_{SS}(\rho^{d}_{SI} + \rho^{d}_{II}) \\
&\quad + f_2 \mu_1 \rho^{d}_{II} - f_1 \beta_1 \langle k_2 \rangle \rho^{d}_{SI}(\rho^{d}_{IS} + \rho^{d}_{II}), \\
\rho^{d}_{II}(t+1) &= \rho^{d}_{II} + f_1 \beta_2 \langle k_2 \rangle \rho^{d}_{IS}(\rho^{d}_{SI} + \rho^{d}_{II}) - f_2 \mu_2 \rho^{d}_{II} \\
&\quad + f_1 \beta_1 \langle k_2 \rangle \rho^{d}_{SI}(\rho^{d}_{IS} + \rho^{d}_{II}) - f_2 \mu_1 \rho^{d}_{II}.
\end{aligned} \tag{3}$$

In the jumping process, we have

$$\begin{aligned}
\rho^{u}_{SS}(t+2) &= (1-\alpha_1)\rho^{u}_{SS}(t+1) + \alpha_1 \rho^{d}_{SS}(t+1), \\
\rho^{u}_{IS}(t+2) &= (1-\alpha_1)\rho^{u}_{IS}(t+1) + \alpha_1 \rho^{d}_{IS}(t+1), \\
\rho^{u}_{SI}(t+2) &= (1-\alpha_1)\rho^{u}_{SI}(t+1) + \alpha_1 \rho^{d}_{SI}(t+1), \\
\rho^{u}_{II}(t+2) &= (1-\alpha_1)\rho^{u}_{II}(t+1) + \alpha_1 \rho^{d}_{II}(t+1)
\end{aligned} \tag{4}$$

for the up layer, where $N^{u} = N_1 - m/2$ and $\alpha_1 = mp/2N^{u}$ represents the density variation caused by the jumping propagators. Similarly, we have

$$\begin{aligned}
\rho^{d}_{SS}(t+2) &= (1-\alpha_2)\rho^{d}_{SS}(t+1) + \alpha_2 \rho^{u}_{SS}(t+1), \\
\rho^{d}_{IS}(t+2) &= (1-\alpha_2)\rho^{d}_{IS}(t+1) + \alpha_2 \rho^{u}_{IS}(t+1), \\
\rho^{d}_{SI}(t+2) &= (1-\alpha_2)\rho^{d}_{SI}(t+1) + \alpha_2 \rho^{u}_{SI}(t+1), \\
\rho^{d}_{II}(t+2) &= (1-\alpha_2)\rho^{d}_{II}(t+1) + \alpha_2 \rho^{u}_{II}(t+1)
\end{aligned} \tag{5}$$

for the down layer, where $N^{d} = N_2 - m/2$ and $\alpha_2 = mp/2N^{d}$. When the system arrives at a stationary state, we have $\rho^{u}_{SS}(t+2) = \rho^{u}_{SS}(t)$, $\rho^{u}_{IS}(t+2) = \rho^{u}_{IS}(t)$, and so on. Substituting them into Eqs. (4) and (5) we have

$$\begin{aligned}
\rho^{u}_{X}(t+1) &= \rho^{u}_{X}(t) + \alpha_1 \xi_X, \\
\rho^{d}_{X}(t+1) &= \rho^{d}_{X}(t) - \alpha_2 \xi_X,
\end{aligned} \tag{6}$$

with $X = \mathrm{SS}$, IS, SI, and II, respectively, and $\xi_X = \rho_X^{\mathrm{u}}(t+1) - \rho_X^{\mathrm{d}}(t+1)$. Substituting them into Eqs. (2) and (3) we have the self-consistent equations

$$\begin{aligned}
\alpha_1\xi_{\mathrm{SS}} &= \mu_1\rho_{\mathrm{IS}}^{\mathrm{u}} + \mu_2\rho_{\mathrm{SI}}^{\mathrm{u}} \\
&\quad - \langle k_1\rangle\rho_{\mathrm{SS}}^{\mathrm{u}}[\beta_1(\rho_{\mathrm{IS}}^{\mathrm{u}} + \rho_{\mathrm{II}}^{\mathrm{u}}) + \beta_2(\rho_{\mathrm{SI}}^{\mathrm{u}} + \rho_{\mathrm{II}}^{\mathrm{u}})], \\
\alpha_1\xi_{\mathrm{IS}} &= -\mu_1\rho_{\mathrm{IS}}^{\mathrm{u}} + \beta_1\langle k_1\rangle\rho_{\mathrm{SS}}^{\mathrm{u}}(\rho_{\mathrm{IS}}^{\mathrm{u}} + \rho_{\mathrm{II}}^{\mathrm{u}}) \\
&\quad + f_2\mu_2\rho_{\mathrm{II}}^{\mathrm{u}} - f_1\beta_2\langle k_1\rangle\rho_{\mathrm{IS}}^{\mathrm{u}}(\rho_{\mathrm{SI}}^{\mathrm{u}} + \rho_{\mathrm{II}}^{\mathrm{u}}), \\
\alpha_1\xi_{\mathrm{SI}} &= -\mu_2\rho_{\mathrm{SI}}^{\mathrm{u}} + \beta_2\langle k_1\rangle\rho_{\mathrm{SS}}^{\mathrm{u}}(\rho_{\mathrm{SI}}^{\mathrm{u}} + \rho_{\mathrm{II}}^{\mathrm{u}}) \\
&\quad + f_2\mu_1\rho_{\mathrm{II}}^{\mathrm{u}} - f_1\beta_1\langle k_1\rangle\rho_{\mathrm{SI}}^{\mathrm{u}}(\rho_{\mathrm{IS}}^{\mathrm{u}} + \rho_{\mathrm{II}}^{\mathrm{u}}), \\
\alpha_1\xi_{\mathrm{II}} &= f_1\beta_2\langle k_1\rangle\rho_{\mathrm{IS}}^{\mathrm{u}}(\rho_{\mathrm{SI}}^{\mathrm{u}} + \rho_{\mathrm{II}}^{\mathrm{u}}) - f_2\mu_2\rho_{\mathrm{II}}^{\mathrm{u}} \\
&\quad + f_1\beta_1\langle k_1\rangle\rho_{\mathrm{SI}}^{\mathrm{u}}(\rho_{\mathrm{IS}}^{\mathrm{u}} + \rho_{\mathrm{II}}^{\mathrm{u}}) - f_2\mu_1\rho_{\mathrm{II}}^{\mathrm{u}}, \qquad (7)
\end{aligned}$$

and

$$\begin{aligned}
-\alpha_2\xi_{\mathrm{SS}} &= \mu_1\rho_{\mathrm{IS}}^{\mathrm{d}} + \mu_2\rho_{\mathrm{SI}}^{\mathrm{d}} \\
&\quad - \langle k_2\rangle\rho_{\mathrm{SS}}^{\mathrm{d}}[\beta_1(\rho_{\mathrm{IS}}^{\mathrm{d}} + \rho_{\mathrm{II}}^{\mathrm{d}}) + \beta_2(\rho_{\mathrm{SI}}^{\mathrm{d}} + \rho_{\mathrm{II}}^{\mathrm{d}})], \\
-\alpha_2\xi_{\mathrm{IS}} &= -\mu_1\rho_{\mathrm{IS}}^{\mathrm{d}} + \beta_1\langle k_2\rangle\rho_{\mathrm{SS}}^{\mathrm{d}}(\rho_{\mathrm{IS}}^{\mathrm{d}} + \rho_{\mathrm{II}}^{\mathrm{d}}) \\
&\quad + f_2\mu_2\rho_{\mathrm{II}}^{\mathrm{d}} - f_1\beta_2\langle k_2\rangle\rho_{\mathrm{IS}}^{\mathrm{d}}(\rho_{\mathrm{SI}}^{\mathrm{d}} + \rho_{\mathrm{II}}^{\mathrm{d}}), \\
-\alpha_2\xi_{\mathrm{SI}} &= -\mu_2\rho_{\mathrm{SI}}^{\mathrm{d}} + \beta_2\langle k_2\rangle\rho_{\mathrm{SS}}^{\mathrm{d}}(\rho_{\mathrm{SI}}^{\mathrm{d}} + \rho_{\mathrm{II}}^{\mathrm{d}}) \\
&\quad + f_2\mu_1\rho_{\mathrm{II}}^{\mathrm{d}} - f_1\beta_1\langle k_2\rangle\rho_{\mathrm{SI}}^{\mathrm{d}}(\rho_{\mathrm{IS}}^{\mathrm{d}} + \rho_{\mathrm{II}}^{\mathrm{d}}), \\
-\alpha_2\xi_{\mathrm{II}} &= f_1\beta_2\langle k_2\rangle\rho_{\mathrm{IS}}^{\mathrm{d}}(\rho_{\mathrm{SI}}^{\mathrm{d}} + \rho_{\mathrm{II}}^{\mathrm{d}}) - f_2\mu_2\rho_{\mathrm{II}}^{\mathrm{d}} \\
&\quad + f_1\beta_1\langle k_2\rangle\rho_{\mathrm{SI}}^{\mathrm{d}}(\rho_{\mathrm{IS}}^{\mathrm{d}} + \rho_{\mathrm{II}}^{\mathrm{d}}) - f_2\mu_1\rho_{\mathrm{II}}^{\mathrm{d}}. \qquad (8)
\end{aligned}$$

The nonlinear algebraic equations (7) and (8) are our final results. To compare them with the obtained numerical results, we first consider the specific case of one pathogen such as $\beta_2 = 0$. From Eq. (6) we have

$$\frac{1}{\alpha_1}(\rho_X^{\mathrm{u}}(t+1) - \rho_X^{\mathrm{u}}(t)) + \frac{1}{\alpha_2}(\rho_X^{\mathrm{d}}(t+1) - \rho_X^{\mathrm{d}}(t)) = 0.$$

Substituting it into Eqs. (7) and (8) and letting $\beta_2 = 0$ we have

$$\begin{aligned}
&\alpha_1\rho_{\mathrm{IS}}^{\mathrm{d}}[\beta_1\langle k_2\rangle(1-\rho_{\mathrm{IS}}^{\mathrm{d}}) - \mu_1] \\
&+ \alpha_2\rho_{\mathrm{IS}}^{\mathrm{u}}[\beta_1\langle k_1\rangle(1-\rho_{\mathrm{IS}}^{\mathrm{u}}) - \mu_1] = 0. \qquad (9)
\end{aligned}$$

When $\rho_{\mathrm{IS}}^{\mathrm{d}} = 0$, the epidemic can spread out only on the up layer and equation (9) thus gives

$$\rho_{\mathrm{IS}}^{\mathrm{u}} = 1 - \frac{\mu_1}{\beta_1\langle k_1\rangle}. \qquad (10)$$

Equation (10) gives the threshold $\beta_{1\mathrm{c}} = \mu_1/\langle k_1\rangle$, which is exactly the threshold in an isolated SIS random network.[66]

For a general solution of the nonlinear algebraic equations (7) and (8), we have two ways to obtain it. The first one is to calculate the fixed point of Eqs. (7) and (8) by the Newton–Raphson method or other similar ones. The second one will start with the initial conditions of $\rho_{\mathrm{SS}}^{\mathrm{u}}(0) \approx 1$, $\rho_{\mathrm{IS}}^{\mathrm{u}}(0) \approx 0$, $\rho_{\mathrm{SI}}^{\mathrm{u}}(0) = 0$, $\rho_{\mathrm{II}}^{\mathrm{u}}(0) = 0$, and $\rho_{\mathrm{SS}}^{\mathrm{d}}(0) \approx 1$, $\rho_{\mathrm{IS}}^{\mathrm{d}}(0) = 0$, $\rho_{\mathrm{SI}}^{\mathrm{d}}(0) \approx 0$, $\rho_{\mathrm{II}}^{\mathrm{d}}(0) = 0$, and then iterate Eqs. (2)–(5) until a steady state is reached. We here use the second way to get the solution. For each set of parameters chosen, we first figure out the values of $\langle k_1\rangle$ and $\langle k_2\rangle$ by counting the total links of the active nodes and making average on time. Then, we substitute them into Eqs. (2)–(5) and focus on the thresholds $\beta_{1\mathrm{c}}$ and $\beta_{2\mathrm{c}}$. The "circles" and "down triangles" in Fig. 5(a)–5(d) represent the theoretical results. Comparing them with the corresponding numerical results, we see that they are consistent with each other very well. After the same process, we can obtain $\beta_{1\mathrm{c}}$ and $\beta_{2\mathrm{c}}$ for different m, see the "circles" and "downtriangles" in Figs. 6(a) and 6(b). Clearly, they are also consistent with the corresponding numerical results very well.

5. Discussion and conclusions

The present study is for the interaction between two SIS pathogens, but it can be easily extended to other cases such as two SIR pathogens, one SIS and one SIR pathogens, or even more than two pathogens. Further, our model can also be extended to the case of traveling between different cities where the travelers take the role of propagators. Although this work is the primary try to consider the role of propagators, its further studies may provide guiding to human mobility patterns and thus may help public health services understand and control human infectious diseases.

In conclusion, we have presented a model of two interactive pathogens in two-layered networks where the connection between the two layers is implemented by a small fraction of propagators. We interestingly find a reverse-feeding phenomenon that the stabilized epidemic spreading on one layer can be sustained by the persistent jumping of propagators from the other layer. When focusing on the thresholds with $p > 0$, we find that the jumping and the mutual interaction between the two pathogens will reduce both $\beta_{\mathrm{c}1}$ and $\beta_{\mathrm{c}2}$. We further show that the reduced epidemic thresholds come mainly from two aspects. One is the different average degrees between the two layers. The other is the modified immune system of the secondary infection, which can be characterized by the factors of f_1 and f_2. A mean-field theory is provided to explain the underlying mechanism of the epidemic spreading in the model. This work provides significant implications for controlling epidemic spreading in realistic cases.

References

[1] Anderson R M and May R M 1991 *Infectious diseases of humans: dynamics and control* (Oxford, New York: Oxford University Press)
[2] Albert R and Barabási A L 2002 *Rev. Mod. Phys.* **74** 47
[3] Dorogovtsev S N, Goltsev A V and Mendes J F F 2008 *Rev. Mod. Phys.* **80** 1275
[4] Pastor-Satorras R and Vespignani A 2001 *Phys. Rev. Lett.* **86** 3200
[5] Eguiluz V M and Klemm K 2002 *Phys. Rev. Lett.* **89** 108701
[6] Newman M E J 2002 *Phys. Rev. E* **66** 016128
[7] Boguna M, Pastor-Satorras R and Vespignani A 2003 *Phys. Rev. Lett.* **90** 028701

[8] Gross T, D'Lima C J D and Blasius B 2006 *Phys. Rev. Lett.* **96** 208701
[9] Parshani R, Carmi S and Havlin S 2010 *Phys. Rev. Lett.* **104** 258701
[10] Castellano C and Pastor-Satorras R 2010 *Phys. Rev. Lett.* **105** 218701
[11] Schwarzkopf Y, Rakos A and Mukamel D 2010 *Phys. Rev. E* **82** 036112
[12] Pastor-Satorras R and Vespignani A 2002 *Phys. Rev. E* **65** 036104
[13] Dezso Z and Barabasi A L 2002 *Phys. Rev. E* **65** 055103
[14] Liu Z, Lai Y C and Ye N 2003 *Phys. Rev. E* **67** 031911
[15] Cohen R, Havlin S and ben-Avraham D 2003 *Phys. Rev. Lett.* **91** 247901
[16] Gallos L K *et al.* 2007 *Phys. Rev. E* **75** 045104(R)
[17] Ferguson N 2007 *Nature* **446** 12
[18] Meloni S *et al.* 2011 *Sci. Rep.* **1** 62
[19] Schwartz I B and Shaw L B 2010 *Physics* **3** 17
[20] Ruan Z, Tang M and Liu Z 2012 *Phys. Rev. E* **86** 036117
[21] Li K, Xu Z, Zhu G and Ding Y 2014 *Chin. Phys. B* **23** 118904
[22] Wang W, Tang M, Yang H, Do Y, Lai Y and Lee G W 2014 *Sci. Rep.* **4** 5097
[23] Liu Q, Wang W, Tang M and Zhang H 2015 arXiv: 1509.08183
[24] Tang M, Liu Z and Li B 2009 *Europhys. Lett.* **87** 18005
[25] Liu Z 2010 *Phys. Rev. E* **81** 016110
[26] Ruan Z, Hui P M, Lin H Q and Liu Z 2013 *Eur. Phys. J. B* **86** 13
[27] Ruan Z, Tang M and Liu Z 2013 *Eur. Phys. J. B* **86** 149
[28] Grassberger P 2013 *J. Stat. Mech.* **2013** 04004
[29] Colizza V, Pastor-Satorras R and Vespignani A 2007 *Nat. Phys.* **3** 276
[30] Colizza V and Vespignani A 2007 *Phys. Rev. Lett.* **99** 148701
[31] Colizza V and Vespignani A 2008 *J. Theor. Biol.* **251** 450
[32] Baronchelli A, Catanzaro M and Pastor-Satorras R 2008 *Phys. Rev. E* **78** 016111
[33] Tang M, Liu L and Liu Z 2009 *Phys. Rev. E* **79** 016108
[34] Wang Z, Wang L and Perc M 2014 *Phys. Rev. E* **89** 052813
[35] Chen Z, Du W, Cao X and Zhou X 2015 *Chaos, Solitons and Fractals* **80** 7
[36] Du W, Zhou X, Chen Z, Cai K and Cao X 2014 *Chaos, Solitons and Fractals* **68** 72
[37] Chen L, Ghanbarnejad F, Cai W and Grassberger P 2013 *Europhys. Lett.* **104** 50001
[38] Mills H L, Ganesh A and Colijn C 2013 *J. Theor. Biol.* **320** 47
[39] Funk S and Jansen V A A 2010 *Phys. Rev. E* **81** 036118
[40] Dickison M, Havlin S and Stanley H E 2012 *Phys. Rev. E* **85** 066109
[41] Saumell-Mendiola A, Serrano M A and Boguna M 2012 *Phys. Rev. E* **86** 026106
[42] Newman M E J 2005 *Phys. Rev. Lett.* **95** 108701
[43] Sulkowski M S 2008 *J. Hepatol.* **48** 353
[44] Abu-Raddad L J, Patnaik P and Kublin J G 2006 *Science* **314** 1603
[45] Brundage J F and Shanks G D 2008 *Emerg. Infect. Dis.* **14** 1193
[46] Oei W and Nishiura H 2012 *Comput. Math. Methods Med.* **2012** 124861
[47] Martcheva M and Pilyugin S S 2006 *SIAM J. Appl. Math.* **66** 843
[48] Marceau V, Noel P A, Hebert-Dufresne L, Allard A and Dube L J 2011 *Phys. Rev. E* **84** 026105
[49] Miller J C 2013 *Phys. Rev. E* **87** 060801
[50] Newman M E J and Ferrario C R 2013 *PLoS ONE* **8** e71321
[51] Britton T, Nordvik M K and Liljeros F 2007 *Theor. Popul. Biol.* **72** 389
[52] Liljeros F, Edling C R, Amaral L A N, Stanley H E and Aberg Y 2001 *Nature* **411** 907
[53] Sanz J, Xia C, Meloni S and Moreno Y 2014 *Phys. Rev. X* **4** 041005
[54] Zhao Y, Zheng M and Liu Z 2014 *Chaos* **24** 043129
[55] Goodenow C, Netherland J and Szalacha L 2002 *Amer. J. Public Health* **92** 203
[56] Hightow L B, Leone P A, Macdonald P D, McCoy S I, Sampson L A and Kaplan A H 2006 *Sexu. Trans. Diseases* **33** 585
[57] Jeffries W L 2011 *Perspect. Sex. Reprod Health* **43** 151
[58] Jeffries W L and Dodge B 2007 *J. Sex Research* **44** 278
[59] Bauch C T and Galvani A P 2013 *Science* **342** 47
[60] Olinky R and Stone L 2004 *Phys. Rev. E* **70** 030902
[61] Liu Z and Hu B 2005 *Europhys. Lett.* **72** 315
[62] Wu Q, Fu X, Small M and Xu X J 2012 *Chaos* **22** 013101
[63] Cai C, Wu Z X and Guan J 2014 *Chaos, Solitons and Fractals* **62–63** 36
[64] Lacroix R, Mukabana W R, Gouagna L C and Koella J C 2005 *PLoS Biol.* **3** e298
[65] Zhou J, Chung N, Chew L and Lai C 2012 *Phys. Rev. E* **86** 026115
[66] Pastor-Satorras R and Vespignani A 2001 *Phys. Rev. E* **63** 066117